5-gene differential expression predicts stability of human intestinal allografts

Paloma Talayero, Lola Alonso-Guirado, Guillermo Padilla, Haydee Artaza, Ana Dopazo, Fátima Sánchez-Cabo, Sarbelio Rodríguez-Muñoz, Jorge Calvo-Pulido, Esther Mancebo, Mario García de Lacoba, Estela Paz-Artal

PII: S0014-4800(17)30297-6
DOI: doi: 10.1016/j.yexmp.2017.08.008
Reference: YEXMP 4076

To appear in: *Experimental and Molecular Pathology*

Received date: 23 May 2017
Revised date: 25 July 2017
Accepted date: 19 August 2017

Please cite this article as: Paloma Talayero, Lola Alonso-Guirado, Guillermo Padilla, Haydee Artaza, Ana Dopazo, Fátima Sánchez-Cabo, Sarbelio Rodríguez-Muñoz, Jorge Calvo-Pulido, Esther Mancebo, Mario García de Lacoba, Estela Paz-Artal , 5-gene differential expression predicts stability of human intestinal allografts. The address for the corresponding author was captured as affiliation for all authors. Please check if appropriate. Yexmp(2017), doi: 10.1016/j.yexmp.2017.08.008

5-gene differential expression predicts stability of human intestinal allografts

Paloma Talayero[1,2], Lola Alonso-Guirado[3], Guillermo Padilla[3], Haydee Artaza[3], Ana Dopazo[4], Fátima Sánchez-Cabo[5], Sarbelio Rodríguez-Muñoz[6], Jorge Calvo-Pulido[7], Esther Mancebo[1,2,8], Mario García de Lacoba[3], Estela Paz-Artal[1,2,8,9]

[1] Department of Immunology, University Hospital 12 de Octubre, Madrid, Spain

[2] I+12 Research Institute, University Hospital 12 de Octubre, Madrid, Spain

[3] Bioinformatics and Biostatistics Unit, Centro de Investigaciones Biológicas (CIB-CSIC), Madrid, Spain

[4] Genomics Unit, Centro Nacional de Investigaciones Cardiovasculares (CNIC), Madrid, Spain

[5] Bioinformatics Unit, Centro Nacional de Investigaciones Cardiovasculares (CNIC), Madrid, Spain

[6] Department of Gastroenterology, University Hospital 12 de Octubre, Madrid, Spain

[7] Department of General and Digestive Surgery and Abdominal Organ Transplantation, University Hospital 12 de Octubre, Madrid, Spain

[8] School of Medicine, Complutense University, Madrid, Spain

[9] Section of Immunology, San Pablo CEU University, Madrid, Spain

Corresponding author: Estela Paz-Artal. Avenida de Córdoba s/n, 28041, Madrid, Spain. estela.paz@salud.madrid.org. +34 917792755.

Abstract:

In intestinal allografts, endoscopy and histology detect the injury once changes in the bowel wall architecture have occurred. We aimed to identify a molecular signature that could predict early deterioration, within histologically indistinguishable biopsies with "minimal changes" (MC) pathology. Sixty biopsies from 12 adult recipients were longitudinally taken during 8 years post-transplant. They were classified as either stable (STA) or non-stable (NSTA) according to the prospectively recorded number, frequency and severity of rejection events of the allograft. In a discovery set of MC samples analyzed by RNA-Seq, 816 genes were differentially expressed in STA vs NSTA biopsies. A group of 5 genes (ADH1C, SLC39A4, CYP4F2, OPTN and PDZK1) correctly classified all NSTA biopsies in the discovery set and all STA biopsies from an independent set. These results were validated by qPCR in a new group of MC biopsies. Based on a logistic regression model, a cutoff of 0.28 predicted the probability of being a NSTA biopsy with 85% sensitivity and 69% specificity. In conclusion, by analyzing MC samples early after transplantation, the expression of a 5-gene set may predict the evolution of the bowel allograft. This prognostic biomarker may be of help to personalize care of the intestinal transplant recipient.

Highlights:

- RNA-Sequencing is a highly sensitive tool for biomarker discovery.
- Apparently histologically equal biopsies are molecularly different.
- A 5-gene signature may be able to predict intestinal graft stability.

Keywords: intestinal transplantation; graft stability; gene expression; RNA-sequencing; biomarkers.

Abbreviations: AUC, area under the curve; CI, confidence interval; cpm, counts per million; DEGs, differencial expressed genes; FDR, false discovery rate; GLM, generalized linear model; IRX, indeterminate for rejection; IT, intestinal transplantation; MC, minimal changes; MDS, multidimensional scaling; NSC, nearest shrunken centroids; NSTA, non-stable; qPCR, quantitative polymerase chain reaction; RF, random forest; RNA-Seq, RNA sequencing; RX, rejection; SBT, small bowel transplantation; STA, stable; SVM, support vector machine; Tx, transplant.

Introduction

Intestinal transplantation (IT) is a procedure to treat irreversible intestinal failure (caused in most cases by ~~a~~ short bowel syndrome) in patients suffering life-threatening complications of parenteral nutrition. Until 2014, nearly 2500 ITx cases had been performed throughout the world, but despite recent improvements, management of IT recipients is still challenging (Grant et al., 2015; Kubal et al., 2015; Smith et al., 2017; Sudan, 2014). In contrast to other organs, the transplanted small bowel bears an important proportion of immune cells and commensal bacterial flora, making it prone to inflammation and infection. The acute rejection rate of intestinal allografts is higher than in other organs and may appear early after transplantation and repeatedly with time (Ruiz, 2012). Severe rejection episodes involve immune mechanisms that eventually damage the intestinal absorptive capacity and favor the translocation of luminal bacteria, which are closely associated with graft loss and patient death. Other post-transplant (post-Tx) events such as lymphoproliferative disease, graft versus host disease, ulcers, enteritis, eosinophilic syndromes or *de novo* autoimmunity, derive from a complex interplay of both non-immune and immune factors as yet barely understood (Fishbein, 2009; Kroemer et al., 2016; Loo et al., 2017; Ranganathan et al., 2015; Selvaggi et al., 2007).

Monitoring of IT integrity relies on endoscopic and histological examination of intestinal mucosa biopsies, continuously performed during the first post-Tx period. However, in a recent series investigating 1770 endoscopies in pediatric transplants, 45% of biopsy-proven rejections showed a normal gross appearance, suggesting a low correlation between endoscopy and histology (Yeh et al., 2015). Thus, in many cases, these

procedures detect the problems once tissular changes have occurred, although the responsible molecular mechanisms may significantly precede them.

In the clinical transplantation arena there is a need for predictive biomarkers for allograft evolution. The transcriptome analysis of the transplanted organ was introduced to identify molecular signatures for rejection, tolerance or drug toxicity. These studies aim to translate into the clinical setting by proposing the measurement of a reduced number of differentially expressed genes to anticipate the event and guide therapy. However, most studies show two important limitations. Firstly, because they analyze very selected and distant pathology phenotypes, i.e. normal *vs* acute rejection biopsies, their results do not provide additional information to that already known. Secondly, in all cases gene expression is measured with probe arrays which do not interrogate the whole transcriptome but an *a priori* determined set of transcripts.

In the present work, we aim to identify a molecular signature of IT deterioration before it translates into visible histological injuries. We explored histologically indistinguishable IT biopsies with minimal changes (MC), which corresponded to either stable (STA) or non-stable (NSTA) intestinal transplants. Because of its potential to quantify the complete transcriptome we used massive RNA sequencing (RNA-Seq) to measure differently expressed genes (Marguerat and Bahler, 2010; Wang et al., 2009). With the unprecedented use of this tool for biomarker discovery in transplantation, we identified and validated a 5-gene set as a molecular classifier with a good predictive capacity for the evolution of IT. The measurement of these 5 genes in IT biopsies by quantitative PCR (qPCR) may identify unstable intestinal allografts and guide early therapeutic intervention.

Materials and Methods

Patients, biopsies and study design

The study included 12 adult recipients who had undergone small bowel (SBT) or multivisceral transplantation between 2005 and 2015 in our hospital (Table 1). Biopsies from ileal mucosa were taken at 10-20 cm from ileostomy. Endoscopic and biopsy controls were performed soon after transplantation and at progressively increasing intervals (2 per week during 1st month, 1 per week during 2nd and 3rd months, 1 every two weeks during 4th and 5th months, 1 monthly until the end of the first year, and then once every six months). According to this protocol, biopsies were routinely taken even in the absence of clinical symptoms, and additional endoscopies and biopsies were performed when clinical events appeared. Data from histological diagnosis from paired biopsies (examined by at least two independent pathologists) and immunosuppressive therapy were also collected. MC were considered in biopsies without specific histopathologic changes, closely resembling the features of normal gut. Indeterminate for rejection (IRX) was considered in biopsies with minimal rejection, less than 6 apoptosis in 10 crypts, mild inflammatory infiltrate and edema. Rejection grade 1 (RX) was defined by increased apoptosis in crypts and epithelium, occasional endothelitis and mild villous blunting (Figure S1) (Andreev et al., 2011; Wu et al., 2003).

All patients received alemtuzumab for induction therapy, except P11 (SBT plus kidney recipient) and P12 who received thymoglobulin. The main immunosuppressive drug was tacrolimus in all patients. Mycophenolate mofetil was added in patients P1, P2, P3, P4 and P12 within the first three months post-Tx. P4, P6, P10, P11 and P12 received

everolimus at 2 months, 6 years, 4 years, 8 months and 1 month post-Tx respectively. Corticosteroids were administered because of a rejection episode in P3, P4, P7, P8, P10 and P11 and because of Crohn's disease (P5), adrenal insufficiency (P10) or kidney allograft (P11).

A total of 60 IT biopsies were longitudinally taken between 2011 and 2015 in a post-Tx period of 13 to 3101 days. Fifty biopsies showed MC, 7 were IRX, and 3 showed RX (Table 2). All 50 MC biopsies were classified into two groups. STA group included all biopsies from allografts of patients who had experienced no rejection, and biopsies from patients who rejected, obtained at least 15 days after rejection, if no other event occurred within the next six months. When rejection occurs, 3 boluses of metilprednisolone are administered followed by decreasing doses of prednisone for 5-10 days. By day 15 after the last rejection biopsy, corticosteroids are minimized and patients are considered clinically stable. NSTA group included biopsies obtained between rejection episodes (those occurring less than 6 months apart), together with biopsies collected within 15 days before the first rejection episode. By defining the biopsies under these criteria we hypothesized that biopsies in the STA category may represent quiescent intestines whereas biopsies in the NSTA group may represent intestinal allografts prone to suffer rejection events. This categorization was established prior to analysis.

Figure 1A shows the workflow for biomarker identification and validation. Twenty-four MC samples (discovery and test sets, 17 STA and 7 NSTA) from 8 patients (Figure 1B and Table 2) were analyzed by RNA-Seq. Eighteen biopsies for the discovery set (11 STA and 7 NSTA) were obtained from 4 IT recipients. To minimize differences due to

the intrinsic characteristics of patients, 3 recipients (P2, P3 and P4) were included because they were the only ones with both STA and NSTA biopsies. All biopsies from the fourth patient included in the discovery set (P1) were STA samples, but they were obtained at a post-Tx period matching that of the other 3 recipients (most biopsies taken within the first year post-Tx) (Figure 1B). The other 6 biopsies from the remaining 4 patients (P5, P6, P7 and P8) were used as the test set. These 6 biopsies were all STA and were taken at long post-Tx time (more than two years) (Figure 1B and Table 2). Genes obtained in the RNA-Seq stage as possible biomarkers were validated as predictors by qPCR and logistic regression in a validation set formed by 26 independent biopsies (17 STA and 9 NSTA) from 9 patients. The model was then tested in a rejection set formed by 10 new biopsies (7 IRX and 3 RX) from 4 patients, and in 16 biopsies from the initial discovery set (Figure 1 and Table 2).

Experiments were approved by the institutional review board (CEIC 13/370) and written informed consent was obtained from all patients.

RNA isolation and quality control

Following extraction, intestinal biopsies were immediately submerged in RNAlater solution (Ambion, Austin, TX, USA) and stored at -80ºC. Samples were maintained this way until RNA extraction, which was performed just before sample processing. After tissue disruption with needle and syringe and homogenization with QIAshredder, RNA was isolated and purified with RNeasy Mini Kit (Qiagen, Hilden, Germany). RNA integrity of samples included in RNA-Seq (24) was determined in a 2100 Bioanalyzer

(Agilent Technologies). All samples passed the quality control, showing an RNA integrity number exceeding 7.

RNA-Seq library production and sequencing

Total RNA was input into the TruSeq RNA Sample Preparation v2 Kit (Illumina, San Diego, CA) to construct index-tagged cDNA libraries. The quality, quantity and size distribution of the Illumina libraries were determined using DNA-1000 Kit (Agilent Bioanalyzer). Libraries were sequenced on Genome Analyzer IIx following the standard RNA-Seq protocol with TruSeq SBS Kit v5. Fastq files containing reads for each library were extracted and demultiplexed with Casava v1.8.2 pipeline. Raw data from the 24 RNA-Seq samples have been deposited in NCBI Gene Expression Omnibus (GEO) with number GSE74118.

RNA-Seq data analysis and classifier discovery

Sequencing adapter contaminations and low-quality reads were removed using Cutadapt software v1.6 (Martin, 2011). Resulting reads were aligned to the reference human genome (Ensembl gene-build GRCh37.75) using TopHat2 v2.0.13 (Kim et al., 2013; Trapnell et al., 2012). Gene expression values were calculated as counts using HTSeq v0.6.1 (Anders et al., 2015). Only genes above 1 count per million (cpm) in all samples were considered for statistical analysis. Data were then normalized by trimmed mean of M-values normalization method (TMM) and differences between STA and NSTA groups in the discovery set were tested by a generalized linear model (GLM)

analysis. To reduce error variance, patient identity and treatment with or without corticosteroids were incorporated into the linear predictor model as blocking factors, so their effects could be discarded when comparing biopsies. Both normalization and model fitting were implemented with the R Bioconductor package edgeR (Robinson et al., 2010). Results were considered significant when Benjamini-Hochberg adjusted p-value was < 0,05 (false discovery rate, FDR<5%). Gene classification, training and testing were performed using nearest shrunken centroids (NSC) method with the R Bioconductor package pamr (Hibi et al., 2012; Tibshirani et al., 2002) and support vector machine (SVM), bagSVM and random forest (RF) (Chen and Ishwaran, 2012; Furey et al., 2000; Peng, 2006; Wang and Sarwal, 2015) with the R Bioconductor package MLSeq. BioGPS (Su et al., 2004; Wu et al., 2009) was used to assess the biological significance of the selected genes. A gene was considered tissue-specific if its expression was at least 3-fold higher in a given tissue than the median expression of the gene across all tissues (Khatri et al., 2013; Roedder et al., 2015).

Quantitative real-time Polymerase Chain Reaction (qPCR)

The expression of the 5 genes selected as classifiers (ADH1C, SLC39A4, CYP4F2, OPTN and PDZK1) was measured with predesigned TaqMan Gene Expression assays (Hs02383872_s1, Hs01592433_g1, Hs00426608_m1, Hs00184221_m1, Hs00275727_m1, Hs02758991_g1) on a 7500 Fast Real-Time PCR System (Applied Biosystems, CA, USA) according to manufacturer's instructions for standard runs and final volume of 20 µL. Threshold cycle (Ct) scores were calculated as the average of the triplicates, and they were normalized against Ct scores for the endogenous control

(GAPDH). Relative expression was determined as $2^{-\Delta Ct}$, where ΔCt = Ct gene of interest – Ct endogenous control (Schmittgen and Livak, 2008). To evaluate the performance of the classifiers as a diagnosis test, a logistic regression model with Firth penalization (used to reduce small-sample bias in maximum likelihood estimation) (Firth, 1993; Heinze and Puhr, 2010; Markowetz and Spang, 2005; Wang, 2014) was built with the relative gene expression data of the validation set. Bootstrap operations for confidence interval (CI) were performed with a non-parametric non-stratified resampling and with the percentile method, as previously described (Carpenter and Bithell, 2000). The generated model was then validated in the rejection set and also in 16 samples of the discovery set. R Bioconductor packages logistf (Heinze et al., 2013), pROC (Robin et al., 2011) and Epi (Carstensen et al., 2017) were used for statistical computing.

Data from qPCR and all R scripts are available as Supplementary Materials and Methods in the Mendeley Data Repository.

Results

816 genes are differentially expressed in stable and non-stable biopsies

Tables 1 and 2 summarize the main characteristics of IT recipients and collected biopsies. Figure 1 shows the flowchart and composition of every sample set analyzed. MC biopsies (Figure S1) were classified into STA or NSTA samples according to criteria described in the Materials and Methods section. By analyzing the data obtained from the RNA-Seq of the discovery set we aimed to find differentially expressed genes (DEGs) between STA and NSTA biopsies in spite of all them being MC, histologically

undistinguishable samples. A total of 13333 genes showed more than 1 cpm in all samples. To search for a possible bias in the samples that could negatively affect future differential expression analysis, we performed a multidimensional scaling (MDS) plot of normalized data (Figure S2A). Because the MDS plot showed a bias by patient identification, this was considered as a blocking factor in GLM analysis when computing differential expression. Administration of corticosteroids at the time of collecting the biopsy was also taken into account as a blocking factor, since it is directly related to rejection. We found 816 DEGs between STA and NSTA biopsies (FDR < 5%); 369 of them were downregulated and 447 were upregulated in NSTA group (Figure S2B).

5 classifier genes discriminate STA and NSTA biopsies

To find a gene signature that could discriminate between STA and NSTA biopsies we performed a NSC analysis with the 816 DEGs. A subset of 5 DEGs was obtained: ADH1C (class I alcohol dehydrogenase gamma subunit), SLC39A4 (solute carrier family 39, member 4), CYP4F2 (cytochrome P450, family 4, subfamily F, polypeptide 2), OPTN (optineurin) and PDZK1 (sodium-hydrogen exchanger regulatory factor 3). ADH1C was more expressed and SLC39A4, CYP4F2, OPTN and PDZK1 were downregulated in NSTA biopsies (Figure 2A). These 5 genes classified biopsies of the discovery set in STA and NSTA with an overall error rate of 11%, showing a misclassification of 2 out of 11 STA biopsies as NSTA (Figure 2B and Table S1) whereas, importantly, all NSTA biopsies were correctly classified. When we calculated the probability of being NSTA in the test set (formed by 6 STA samples) with the model built by the NSC method, all biopsies were correctly classified as STA with NSTA

probabilities < 0.01 (Figure 2B). The power of the 5-gene set to predict stability in discovery and test sets (collectively considering all 24 samples) was confirmed by SVM, bagSVM and RF methods, showing an accuracy, specificity and sensitivity of 100% in the discovery set modeling (Table 3). The predictions for the test set were almost perfect, with only one STA sample misclassified as NSTA by RF method. In hierarchical clustering (Figure 2C) samples with different phenotypes clustered separately even if they came from the same patient. Interestingly, samples with the same phenotype from the same patient clustered together, especially if they were close in time (P3_49 and P3_30, P1_92 and P1_33, P5_1874 and P5_1826), which could be considered a good quality control. Principal component analysis (Figure 2D) showed also good segregation of the samples.

Using BioGPS (Khatri et al., 2013), we found that ADH1C, SLC39A4, CYP4F2 and PDZK1 are preferentially expressed in the small bowel. Interestingly, OPTN was found highly expressed in T lymphocytes (especially in CD4+ but also in CD8+ cells), natural killer (NK) and other cells of lymphoid lineage (Figure 3).

qPCR validation of the 5-gene model

In order to validate the results obtained by RNA-Seq and with the aim of developing a possible diagnostic tool, the 5-gene set expression was measured by qPCR in a new independent group of biopsies. This validation set included 26 biopsies (17 STA and 9 NSTA) from 9 patients (Figure 1 and Table 2). A logistic regression model (corrected with Firth penalization to reduce small-sample bias in maximum likelihood estimation) was developed with the GAPDH-normalized 5-gene expression data. Table S2 shows

regression coefficients that describe the size of the contribution of each gene as a risk factor.

Based on the ROC curve built upon this regression model with an AUC of 0.81 (95% CI, 0.63 to 0.96), a cutoff value θ=0.28 classified NSTA and STA samples with 53% specificity and the highest sensitivity (100%) (95% CI, 0.29 to 0.76), and, importantly, it allowed the detection of every NSTA biopsy (Figure 4A). The 5 gene-model was subsequently tested in a set of samples with histological diagnosis of IRX (n=7) or acute rejection (n=3, Table 2), under the hypothesis that it should classify these samples as NSTA. Assuming the same reference value of 0.28 as a classifier score, the model misclassified only one IRX sample and one RX biopsy (the last one with a predicted probability of 0.27) (Figure 4B). Finally, within 16 biopsies from discovery set (9 STA and 7 NSTA) tested by the regression model, only two NSTA samples were misclassified (Figure 4C). Taking together all the results obtained in the three sets of samples (discovery, rejection and validation), the model showed an accuracy of 77% (85% sensitivity, 69% specificity, 73% positive predictive value, 82% negative predictive value).

Figure 4D shows the predicted probabilities in four different patients, those with a higher number of studied biopsies along post-Tx time. Patient 1 never suffered rejection so, with regard to our initial definition, all his 6 biopsies were STA. According to predicted probabilities, only the sample obtained at day 26 post-Tx was misclassified, whereas all other biopsies (from day 33 to 1201 post-Tx) were correctly classified. Within 12 samples from patient 2, only two were misclassified. The first was a RX biopsy taken at day 58 and was classified as STA with a probability value very close to the cutoff (0.27).

The second misclassified biopsy was taken on day 448. This sample, which was diagnosed as IRX, was an isolated biopsy with no previous or later RX or IRX biopsies. The patient did not develop clinical symptoms of rejection and no changes were made in the immunosuppression. Accordingly, this biopsy might well have been classified as MC and STA. Patient 4 suffered several IRX biopsies and many rejection episodes even two years post-Tx. The unstable evolution of his intestinal graft is well reflected by the predicted probabilities that show three misclassifications (within 11 samples analyzed). Patient 12 showed only one misclassification out of 11 samples, corresponding to the biopsy obtained at day 171 (STA). Although this sample was classified as NSTA, its predicted probability was lower than probabilities for the same patient NSTA, RX or IRX biopsies. These examples illustrate that the molecular signature described here may be more accurate than histology to diagnose the status of intestinal allograft. Not only the predicted probability values of isolated samples, but also the trend of probabilities within each patient could be a guide to prognosticate the transplant stability.

Discussion

The design of the present analysis shows three main strengths. Firstly, as opposed to other studies (Bradley et al., 2008), we have not compared clinical distant, rejection *vs* non-rejection biopsies, but we have analyzed an *a priori* histologically homogeneous, all "minimal changes" group of samples. The emerged 5-gene signature is able to accurately identify MC biopsies corresponding to non-stable intestinal transplants which will probably suffer more frequent and more severe rejection events, and MC biopsies corresponding to stable grafts. Secondly, because we found the 5-gene signature in

biopsies showing incipient injury, valuable information has been gained about the molecular mechanisms of early IT deterioration before it translates into visible histological changes. Thirdly, the transcriptome has been profiled by RNA-Seq, a technology that does not explore a predetermined set of transcripts according to an array of probes, but the whole transcriptome. RNA-Seq has shown to be a highly quantitative technology with a wide dynamic range and measures differential gene expression at least as well as microarrays (Marguerat and Bahler, 2010; Wang et al., 2009). On the other hand, IT is a very infrequent clinical procedure and obtaining biopsy samples for research purposes is hampered by sophisticated logistics. The disparity between the sample size and the multidimensionality of the analyzed data needs to be mentioned as a limitation in our study. Nevertheless, classifiers obtained in only 4 patients have been validated in eight different patients set by several methods. In small cohorts, slight inter-individual differences have greater effects, so to standardize and validate the findings has an added value.

We performed a search of the 5 genes reported here across all transplantation-related transcriptomes deposited in GEO. In a study of renal transplants, all 5 genes were more expressed in biopsies from well-functioning grafts than in biopsies from acute rejection or renal dysfunction without rejection (Flechner et al., 2004). This is consistent with changes in the same direction for CYP4F2, PDZK1, SLC39A4 and OPTN in the present study, as these genes were significantly more expressed in STA *vs* NSTA samples.

All 5 genes included in the molecular signature are important for the enteric physiology. ADH1C (also known as ADH3), mediates the synthesis of retinoic acid by metabolizing retinol (Molotkov et al., 2002). Migratory dendritic cells from mesenteric lymph nodes

use retinoic acid to induce the expression of gut homing molecules on T cells and innate lymphoid cells 1 and 3 (Habtezion et al., 2016). The recorded overexpression of ADH1C in NSTA samples might be consistent with an enhanced retinoic acid-mediated lymphocyte traffic into the small intestine, as the first step for the initiation of local effector responses that might disrupt the stability of the allograft.

CYP4F2, which was downregulated in NSTA samples, reduces the activity of several fatty acid metabolites of arachidonic acid, such as leukotriene B4 and prostaglandins, which are potent mediators of inflammation. The role of CYP4F2 in reducing inflammation could be related with the association of certain CYP4F2 single nucleotide variants with Crohn's (Costea et al., 2010) and celiac diseases (Curley et al., 2006). Interestingly, a metabolomics analysis of effluent fluid from ileostomy or stool in IT recipients found that leukotriene E4 showed the highest fold change in rejection compared to non-rejection samples (Girlanda et al., 2012).

PDZK1 expression is limited to epithelial cells. It is a fundamental component in brush borders of renal proximal tubular cells, where it interacts with sodium transporters (Gisler et al., 2003). Recently, PDZK1 mRNA and protein have been shown strongly downregulated in the enterocytes of a model of murine colitis and in ulcerative colitis patients (Lenzen et al., 2012; Yeruva et al., 2015). The decrease of PDZK1 diminishes the sodium/hydrogen ionic transport rate of members of the solute carrier family (SLC) located in the apical membrane of the enterocyte. These observations link intestinal inflammation to molecular disturbances in the enteric physiology. The decrease of PDZK1 in NSTA biopsies may be considered a biomarker of ongoing inflammation in the intestinal graft.

SLC39A4, also known as ZIP4, is abundantly expressed in the apical membrane of the enterocytes. Mutations in SLC39A4 impair zinc absorption and cause acrodermatitis enteropathica (Kury et al., 2002; Yeruva et al., 2015). Insufficient zinc absorption is commonly observed among IT recipients (Ubesie et al., 2013; Venick et al., 2006; Venick et al., 2011). Overexpression of SLC39A4 in hepatocellular or pancreatic carcinomas increases cell growth and represses apoptosis (Weaver et al., 2010; Zhang et al., 2010), while its lack in enterocytic-specific SLC39A4 KO mice causes dysfunction of Paneth cells that leads to disruption of the villus stem cell niche in the crypts. Remarkably, apoptosis and crypts distortion are hallmarks of intestinal allograft rejection (Ruiz et al., 2004; Ruiz et al., 2010).

Within the 5-gene signature, only OPTN is significantly expressed in lymphoid cells. This is biologically consistent with the fact that the inflammatory infiltrate was not a prominent feature in most samples, as they were MC biopsies. Optineurin participates in the autophagy process to limit intracellular proliferation of *Salmonella* (Wild et al., 2011). Mice without OPTN are significantly susceptible to Salmonella infection (Slowicka et al., 2016) and peritonitis caused by *Citrobacter* colitis and *E. coli*, due to reduced neutrophil recruitment to sites of acute inflammation and impaired pro-inflammatory cytokine secretion. (Chew et al., 2015). In a subgroup of patients with Crohn's disease, optineurin was the most common under-expressed transcript in macrophages, which were also defective in production and release of tumor necrosis factor and interferon-γ after stimulation by *E. coli* (Smith et al., 2015). Interestingly, profiling of microbiota in ileal effluents from transplanted intestines showed an increase of taxa from the *Enterobacteriaceae* family during rejection (Oh et al., 2012). These data suggest a role

for optineurin in the innate immune response to bacteria in the gut. A reduced expression of OPTN might negatively impact the evolution of the intestinal allograft by favoring the bacterial overgrow.

In conclusion, we have found a 5-gene expression signature useful as a prognostic classifier for the intestinal grafts that may help to intensify or reduce surveillance biopsies or therapy. The molecular signature can be identified early after transplantation and does not include typical inflammation or effector immune response transcripts, which probably correspond to allografts with prominent infiltration and more advanced injury phases. Thus, the 5-gene set may discriminate, within histologically indistinguishable biopsies, those corresponding to grafts with damage before they translate into visible tissular changes. Given this molecular information, clinical decisions such as the dose adjustment of immunosuppressive drugs or the biopsy monitoring frequency could be taken to prevent and anticipate the allograft damage. Histological findings of intestinal rejection (Ruiz et al., 2004) are not specific and high apoptosis rates can be found in patients receiving mycophenolate mofetil (Apostolov et al., 2017) or during adenovirus infections (Kaufman et al., 2002). As the 5-gene set also identifies RX and IRX biopsies, it could be useful to discriminate those “false rejection” biopsies, avoiding the aggressive anti-rejection therapies. Larger studies of more samples, pediatric patients and a prospective and multicenter design may provide further evidence of our results and confirm their clinical usefulness.

Acknowledgments: We thank Dra. P. López García for the images of the histology of the intestinal biopsies. We also thank the patients for their collaboration in this study.

Funding was obtained from projects 13/00045 and 13/01407 to E. P-A (Instituto de Salud Carlos III, Spain, and European Regional Development Fund) and project 13/0068 to J. C-P (Fundación Mutua Madrileña).

Funding sources: Funding for this study was obtained from projects 13/00045 and 13/01407 to E. P-A (Instituto de Salud Carlos III, Spain, and European Regional Development Fund) and project 13/0068 to J. C-P (Fundación Mutua Madrileña).

Disclosure: The authors declare no conflicts of interest.

References:

Anders, S., et al., 2015. HTSeq--a Python framework to work with high-throughput sequencing data. Bioinformatics. 31**,** 166-9.

Andreev, V. P., et al., 2011. Peripheral blood gene expression analysis in intestinal transplantation: a feasibility study for detecting novel candidate biomarkers of graft rejection. Transplantation. 92**,** 1385-91.

Apostolov, R., et al., 2017. Mycophenolate mofetil toxicity mimicking acute cellular rejection in a small intestinal transplant. World J Transplant. 7**,** 98-102.

Bradley, S. P., et al., 2008. Genetic expression profile during acute cellular rejection in clinical intestinal transplantation. Transplantation. 86**,** 998-1001.

Carpenter, J., Bithell, J., 2000. Bootstrap confidence intervals: when, which, what? A practical guide for medical statisticians. Stat Med. 19**,** 1141-64.

Carstensen, B., et al., Epi: A Package for Statistical Analysis in Epidemiology. 2017.

Costea, I., et al., 2010. Genes involved in the metabolism of poly-unsaturated fatty-acids (PUFA) and risk for Crohn's disease in children & young adults. PLoS One. 5, e15672.

Curley, C. R., et al., 2006. A functional candidate screen for coeliac disease genes. Eur J Hum Genet. 14, 1215-22.

Chen, X., Ishwaran, H., 2012. Random forests for genomic data analysis. Genomics. 99, 323-9.

Chew, T. S., et al., 2015. Optineurin deficiency in mice contributes to impaired cytokine secretion and neutrophil recruitment in bacteria-driven colitis. Dis Model Mech. 8, 817-29.

Firth, D., 1993. Bias reduction of maximum likelihood estimates. Biometrika. 80, 27-38.

Fishbein, T. M., 2009. Intestinal transplantation. N Engl J Med. 361, 998-1008.

Flechner, S. M., et al., 2004. Kidney transplant rejection and tissue injury by gene profiling of biopsies and peripheral blood lymphocytes. Am J Transplant. 4, 1475-89.

Furey, T. S., et al., 2000. Support vector machine classification and validation of cancer tissue samples using microarray expression data. Bioinformatics. 16, 906-14.

Girlanda, R., et al., 2012. Metabolomics of human intestinal transplant rejection. Am J Transplant. 12 Suppl 4, S18-26.

Gisler, S. M., et al., 2003. PDZK1: I. a major scaffolder in brush borders of proximal tubular cells. Kidney Int. 64, 1733-45.

Grant, D., et al., 2015. Intestinal transplant registry report: global activity and trends. Am J Transplant. 15, 210-9.

Habtezion, A., et al., 2016. Leukocyte Trafficking to the Small Intestine and Colon. Gastroenterology. 150, 340-54.

Heinze, G., et al., logistf: Firth's bias reduced logistic regression. 2013.

Heinze, G., Puhr, R., 2010. Bias-reduced and separation-proof conditional logistic regression with small or sparse data sets. Stat Med. 29, 770-7.

Hibi, T., et al., 2012. Citrulline level is a potent indicator of acute rejection in the long term following pediatric intestinal/multivisceral transplantation. Am J Transplant. 12 Suppl 4, S27-32.

Kaufman, S. S., et al., 2002. Discrimination between acute rejection and adenoviral enteritis in intestinal transplant recipients. Transplant Proc. 34, 943-5.

Khatri, P., et al., 2013. A common rejection module (CRM) for acute rejection across multiple organs identifies novel therapeutics for organ transplantation. J Exp Med. 210, 2205-21.

Kim, D., et al., 2013. TopHat2: accurate alignment of transcriptomes in the presence of insertions, deletions and gene fusions. Genome Biol. 14, R36.

Kroemer, A., et al., 2016. Intestinal Transplant Inflammation: the Third Inflammatory Bowel Disease. Curr Gastroenterol Rep. 18, 56.

Kubal, C. A., et al., 2015. Intestine and multivisceral transplantation: current status and future directions. Curr Gastroenterol Rep. 17, 427.

Kury, S., et al., 2002. Identification of SLC39A4, a gene involved in acrodermatitis enteropathica. Nat Genet. 31, 239-40.

Lenzen, H., et al., 2012. Downregulation of the NHE3-binding PDZ-adaptor protein PDZK1 expression during cytokine-induced inflammation in interleukin-10-deficient mice. PLoS One. 7, e40657.

Loo, L., et al., 2017. Intestinal transplantation: a review. Curr Opin Gastroenterol. 33, 203-211.

Marguerat, S., Bahler, J., 2010. RNA-seq: from technology to biology. Cell Mol Life Sci. 67, 569-79.

Markowetz, F., Spang, R., 2005. Molecular diagnosis. Classification, model selection and performance evaluation. Methods Inf Med. 44, 438-43.

Martin, M., 2011. Cutadapt removes adapter sequences from high-throughput sequencing reads. EMBnet.journal. 17, 10-12.

Molotkov, A., et al., 2002. Stimulation of retinoic acid production and growth by ubiquitously expressed alcohol dehydrogenase Adh3. Proc Natl Acad Sci U S A. 99, 5337-42.

Oh, P. L., et al., 2012. Characterization of the ileal microbiota in rejecting and nonrejecting recipients of small bowel transplants. Am J Transplant. 12, 753-62.

Peng, Y., 2006. A novel ensemble machine learning for robust microarray data classification. Comput Biol Med. 36, 553-73.

Ranganathan, S., et al., 2015. The transcription factor, T-bet, primes intestine transplantation rejection and is associated with disrupted mucosal homeostasis. Transplantation. 99, 890-4.

Robin, X., et al., 2011. pROC: an open-source package for R and S+ to analyze and compare ROC curves. BMC Bioinformatics. 12, 77.

Robinson, M. D., et al., 2010. edgeR: a Bioconductor package for differential expression analysis of digital gene expression data. Bioinformatics. 26, 139-40.

Roedder, S., et al., 2015. A Three-Gene Assay for Monitoring Immune Quiescence in Kidney Transplantation. J Am Soc Nephrol. 26, 2042-53.

Ruiz, P., 2012. How can pathologists help to diagnose late complications in small bowel and multivisceral transplantation? Curr Opin Organ Transplant. 17, 273-9.

Ruiz, P., et al., 2004. Histological criteria for the identification of acute cellular rejection in human small bowel allografts: results of the pathology workshop at the VIII International Small Bowel Transplant Symposium. Transplant Proc. 36, 335-7.

Ruiz, P., et al., 2010. International grading scheme for acute cellular rejection in small-bowel transplantation: single-center experience. Transplant Proc. 42, 47-53.

Schmittgen, T. D., Livak, K. J., 2008. Analyzing real-time PCR data by the comparative C(T) method. Nat Protoc. 3, 1101-8.

Selvaggi, G., et al., 2007. Analysis of acute cellular rejection episodes in recipients of primary intestinal transplantation: a single center, 11-year experience. Am J Transplant. 7, 1249-57.

Slowicka, K., et al., 2016. Optineurin deficiency in mice is associated with increased sensitivity to Salmonella but does not affect proinflammatory NF-kappaB signaling. Eur J Immunol. 46, 971-80.

Smith, A. M., et al., 2015. Disruption of macrophage pro-inflammatory cytokine release in Crohn's disease is associated with reduced optineurin expression in a subset of patients. Immunology. 144, 45-55.

Smith, J. M., et al., 2017. OPTN/SRTR 2015 Annual Data Report: Intestine. Am J Transplant. 17 Suppl 1, 252-285.

Su, A. I., et al., 2004. A gene atlas of the mouse and human protein-encoding transcriptomes. Proc Natl Acad Sci U S A. 101, 6062-7.

Sudan, D., 2014. The current state of intestine transplantation: indications, techniques, outcomes and challenges. Am J Transplant. 14, 1976-84.

Tibshirani, R., et al., 2002. Diagnosis of multiple cancer types by shrunken centroids of gene expression. Proc Natl Acad Sci U S A. 99, 6567-72.

Trapnell, C., et al., 2012. Differential gene and transcript expression analysis of RNA-seq experiments with TopHat and Cufflinks. Nat Protoc. 7, 562-78.

Ubesie, A. C., et al., 2013. Micronutrient deficiencies in pediatric and young adult intestinal transplant patients. Pediatr Transplant. 17, 638-45.

Venick, R. S., et al., 2006. Nutritional outcomes following pediatric intestinal transplantation. Transplant Proc. 38, 1718-9.

Venick, R. S., et al., 2011. Long-term nutrition and predictors of growth and weight gain following pediatric intestinal transplantation. Transplantation. 92, 1058-62.

Wang, A., Sarwal, M. M., 2015. Computational Models for Transplant Biomarker Discovery. Front Immunol. 6, 458.

Wang, X., 2014. Firth logistic regression for rare variant association tests. Front Genet. 5, 187.

Wang, Z., et al., 2009. RNA-Seq: a revolutionary tool for transcriptomics. Nat Rev Genet. 10, 57-63.

Weaver, B. P., et al., 2010. Zip4 (Slc39a4) expression is activated in hepatocellular carcinomas and functions to repress apoptosis, enhance cell cycle and increase migration. PLoS One. 5, e13158.

Wild, P., et al., 2011. Phosphorylation of the autophagy receptor optineurin restricts Salmonella growth. Science. 333, 228-33.

Wu, C., et al., 2009. BioGPS: an extensible and customizable portal for querying and organizing gene annotation resources. Genome Biol. 10, R130.

Wu, T., et al., 2003. A schema for histologic grading of small intestine allograft acute rejection. Transplantation. 75, 1241-8.

Yeh, J., et al., 2015. Endoscopy Following Pediatric Intestinal Transplant. J Pediatr Gastroenterol Nutr. 61, 636-40.

Yeruva, S., et al., 2015. Evidence for a causal link between adaptor protein PDZK1 downregulation and Na(+)/H(+) exchanger NHE3 dysfunction in human and murine colitis. Pflugers Arch. 467, 1795-807.

Zhang, Y., et al., 2010. ZIP4 regulates pancreatic cancer cell growth by activating IL-6/STAT3 pathway through zinc finger transcription factor CREB. Clin Cancer Res. 16, 1423-30.

Figure Legends

Figure 1. Workflow of biomarker panel identification and validation, biopsies and patients. (A) In the RNA-Seq stage, the selection of classifier genes was performed with the discovery set, while the test set was used for validation of the results. In the qPCR stage, a logistic regression model was built with the results of a new independent cohort (validation set). The model was tested in the rejection set and re-validated in 16 samples of the discovery set (the remaining 2 samples were not tested because no RNA was available). (B) Graphic representation of studied biopsies along post-transplant time for each patient. Symbols represent biopsy type (STA, NSTA, IRX or RX) and colors show the group where they are included (discovery, test, validation and rejection sets).

Figure 2. Gene selection and prediction based on the 5-gene set RNA-Seq expression values. (A) Expression in cpm of the top five genes selected by NSC method. Each symbol represents a biopsy. NSTA samples are represented by ▲ and STA samples by ●. (B) The probabilities of being NSTA based on the expression of these five genes were calculated for the discovery set (up) and the test set (down). (C) Heatmap and hierarchical clustering (dissimilarities are represented by the Manhattan distance and clusters are defined by the Ward method) in both discovery and test sets show the segregation of STA and NSTA samples. Rows represent genes, and columns represent biopsies. Relative expression values were calculated as standardized z-scores, obtained by the following formula: z-score= (x- mean)/standard deviation, where "x" is the normalized gene expression of each sample. Z-scores were scaled across

rows. Red and blue indicate respectively over- and under-expression of the gene. (D) Principal Component Analysis plot. STA and NSTA samples of discovery and test sets are clearly separated along dimension 1, which explains 67.8% of the differences between both groups.

Figure 3. Tissue-specific patterns of mRNA expression of the 5-genes set. Gene expression profiles of 79 human tissues obtained from the GeneAtlas U133A dataset (BioGPS). It has been proposed that a gene is tissue-specific if its expression is at least 3-fold higher in a given tissue than the median expression of the gene across all tissues.

Figure 4. 5-gene set qPCR validation. (A) ROC curve from the logistic regression model developed with qPCR gene expression data from the discovery set for a probability cutoff θ = 0.28 (up). Performance of the regression model in the validation set (down). (B, C) Predicted probabilities on the rejection set (B) and discovery set (C) biopsies derived from the logistic regression model. Dotted line represents the cutoff value selected (θ = 0.28). (D) Evolution of the predicted probabilities along post-transplant time in four different patients. Biopsies are plotted in the x axis (numbers show the days after transplantation). ● STA, ▲ NSTA, ▼ RX, ◆ IRX.

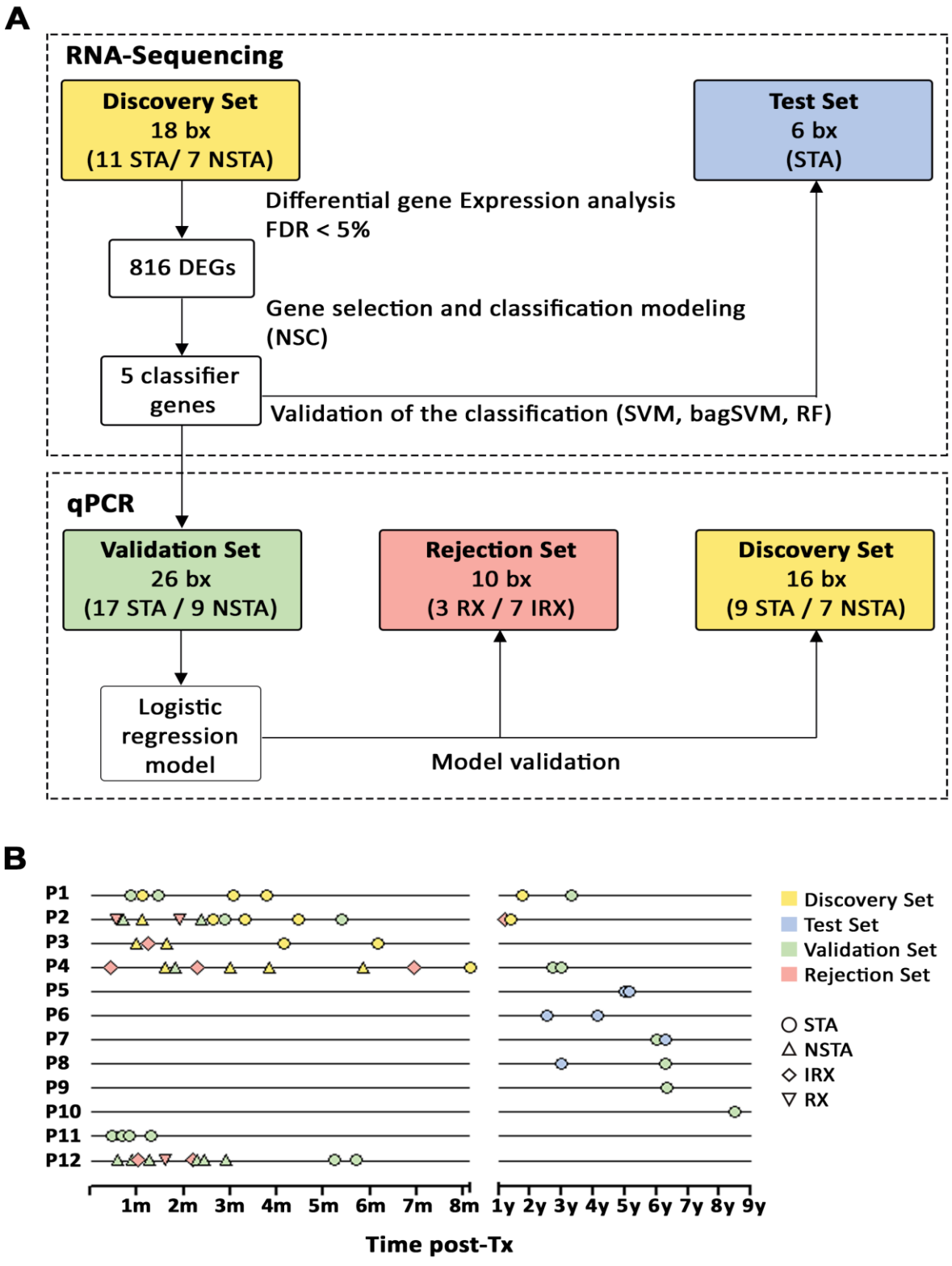

Figure 1

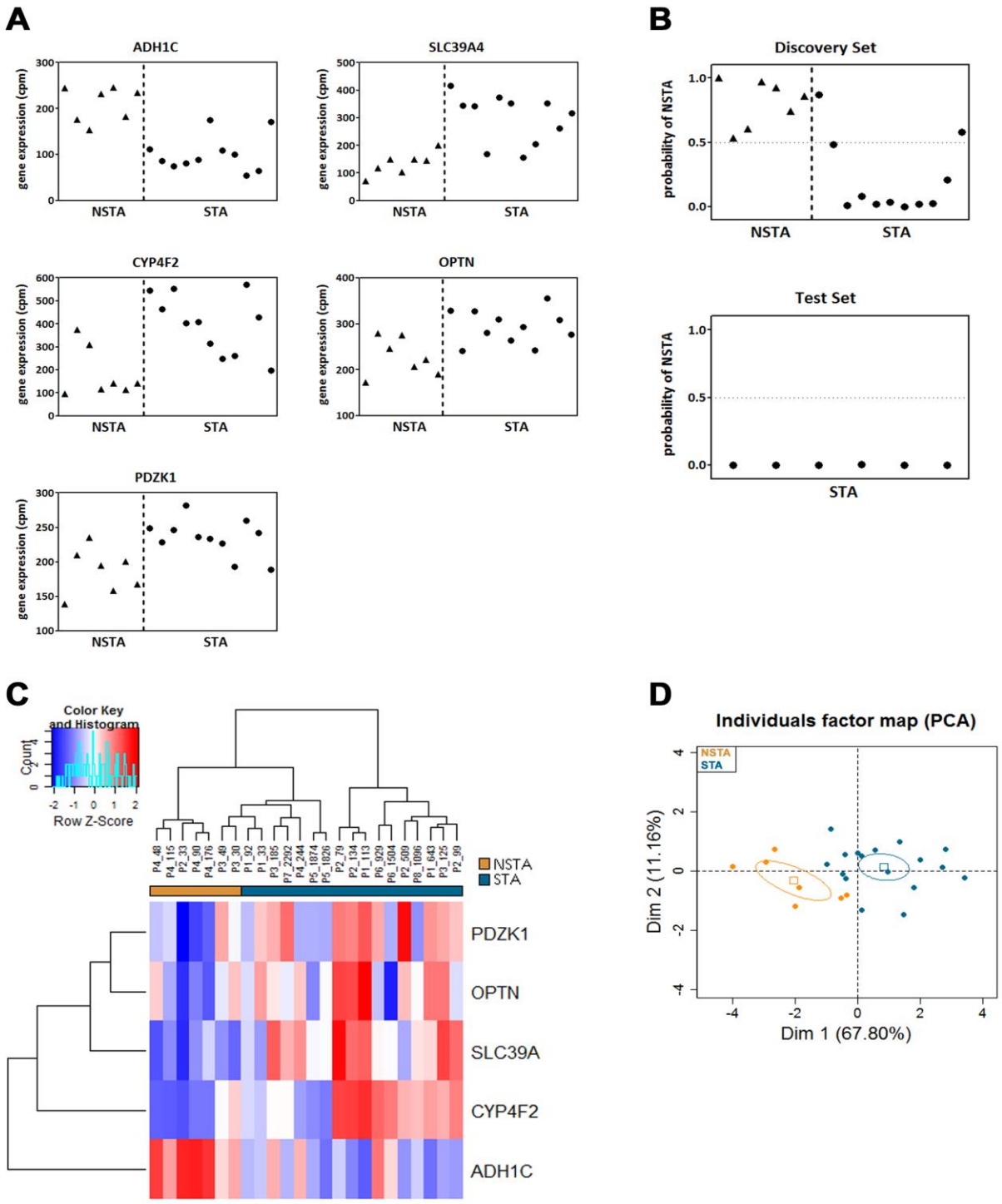

Figure 2

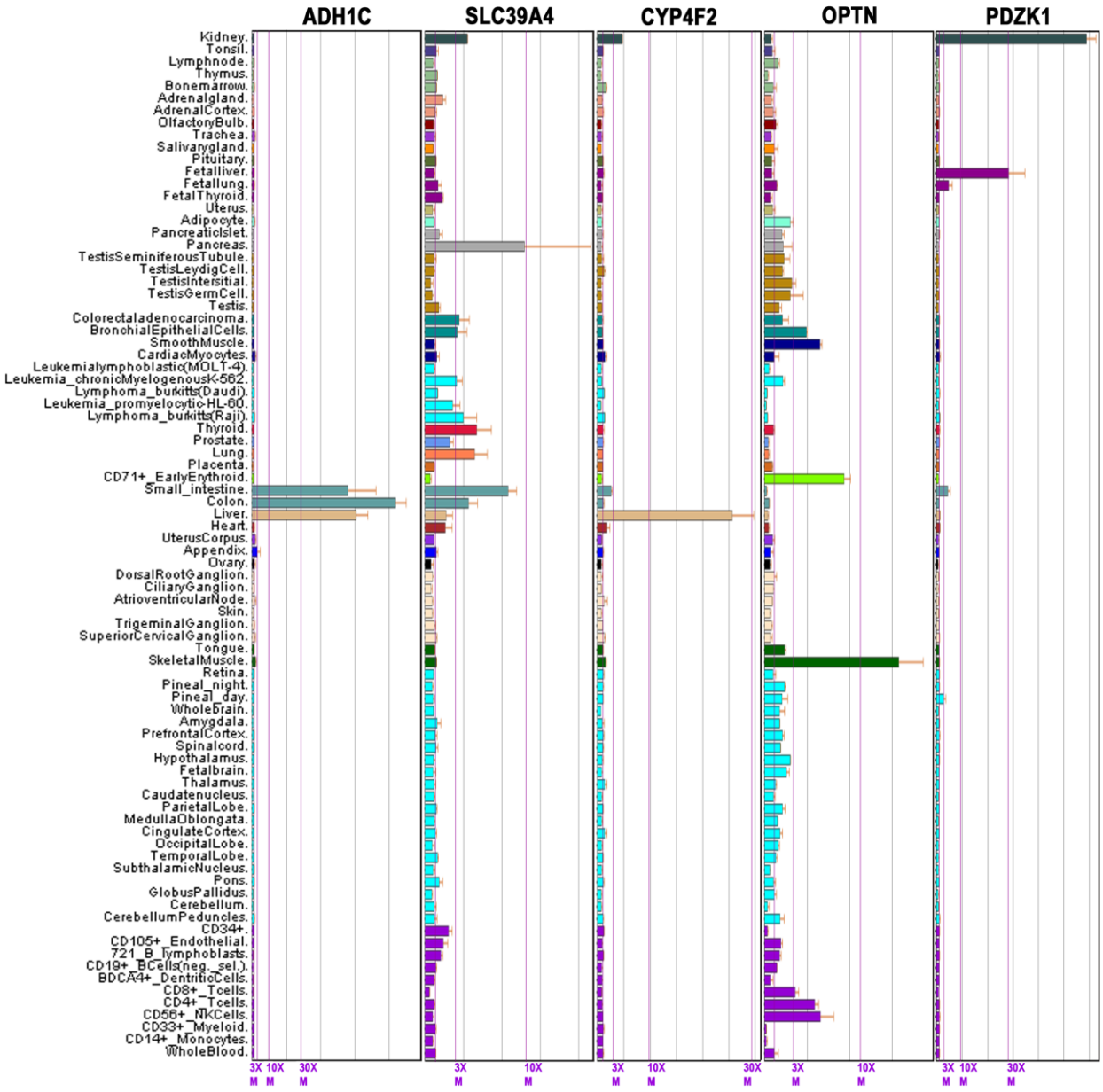

Figure 3

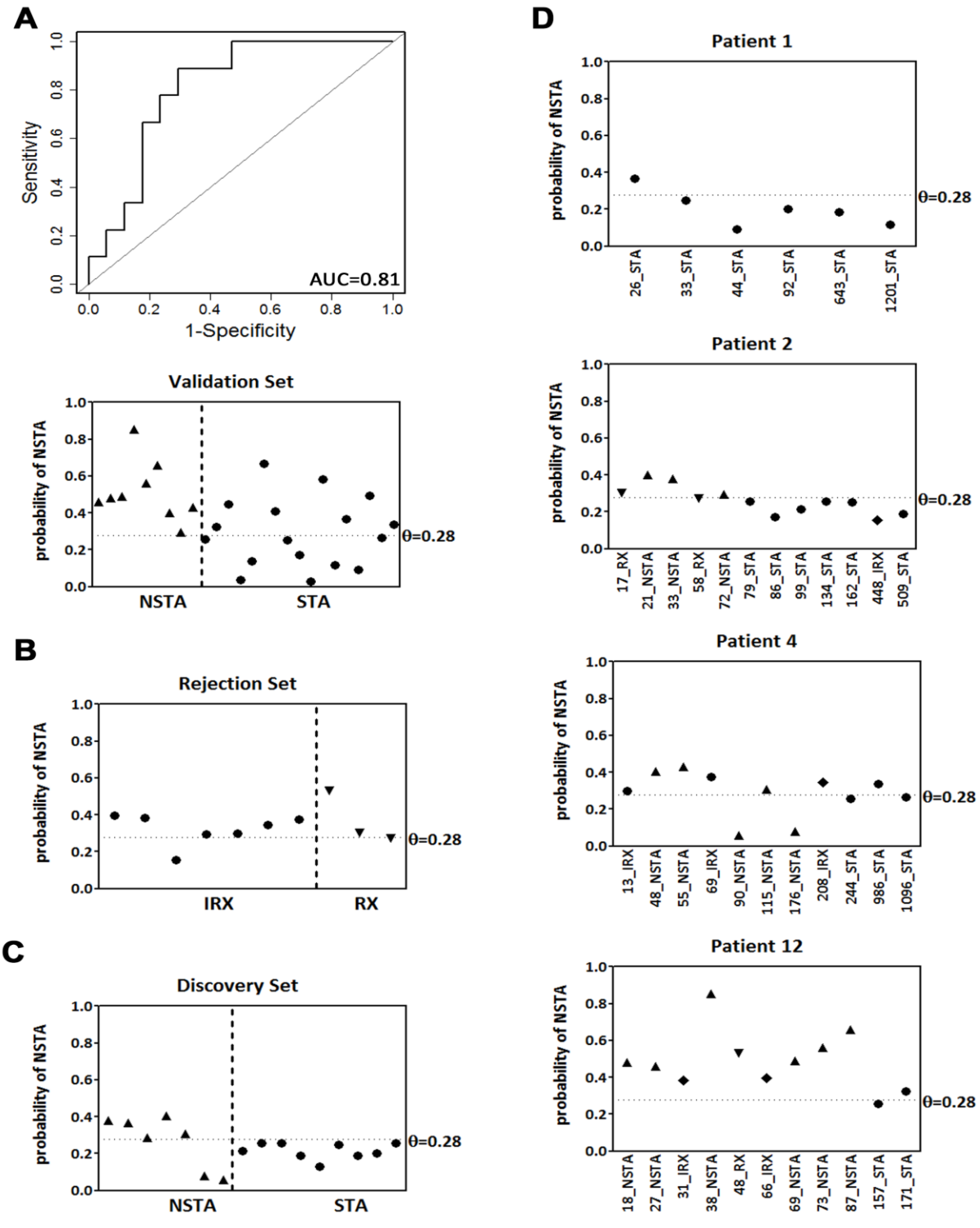

Figure 4

Table 1. Clinical data from small bowel and multivisceral recipients.

Patient	Underlying disease	Gender	Age at Tx	Organ Tx
P1	Familial Adenomatous Polyposis	Male	40	SBT
P2	Familial Adenomatous Polyposis	Male	44	SBT
P3	Familial Adenomatous Polyposis	Male	24	SBT
P4	Acute mesenteric ischemia	Female	38	SBT
P5	Crohn's disease	Male	38	SBT
P6	Acute mesenteric ischemia	Male	64	SBT
P7	Acute mesenteric ischemia	Male	45	SBT
P8	Politraumatism	Male	30	SBT
P9	Gastrointestinal stromal tumor (GIST)	Female	47	SBT
P10	Familial Adenomatous Polyposis	Female	32	MVT
P11	Primary intestinal lymphangiectasia Haemolytic uremic syndrome	Female	26	SBT + Kidney
P12	Intestinal pseudo-obstruction syndrome	Female	30	MVT

Tx: transplantation / SBT: small bowel transplantation / MVT: multivisceral abdominal transplantation

Table 2. Number of biopsies studied according to post-transplantation time.

		RNA-Seq		qPCR	
Patient	**Nº bx**	**Discovery Set**	**Test Set**	**Validation Set**	**Rejection Set**
P1	7	4 STA (33,92,113,643)	---	3 STA (26,44,1201)	---
P2	12	4 STA (79,99,134,509) 1 NSTA (33)	---	2 STA (86,162) 2 NSTA (21,72)	1 IRX (448) 2 RX (17,58)
P3	5	2 STA (125,185) 2 NSTA (30,49)	---	---	1 IRX (37)
P4	11	1 STA (244) 4 NSTA (48,90,115,176)	---	2 STA (986,1096) 1 NSTA (55)	3 IRX (13,69,208)
P5	2	---	2 STA (1826,1874)	---	---
P6	2	---	2 STA (929,1504)	---	---
P7	2	---	1 STA (2292)	1 STA (2202)	---
P8	2	---	1 STA (1096)	1 STA (2297)	---
P9	1	---	---	1 STA (2306)	---
P10	1	---	---	1 STA (3101)	---
P11	4	---	---	4 STA (14,20,25,39)	---
P12	11	---	---	2 STA (157,171) 6 NSTA (18,27,38,69,73,87)	2 IRX (31, 66) 1 RX (48)

Numbers between ( ) represent days post-transplantation / Bx: biopsies / STA: biopsy with minimal changes considered in the stable group / NSTA: biopsy with minimal changes considered in the non-stable group / IRX: biopsy with a diagnosis of indeterminated for rejection / RX: biopsy with a diagnosis of acute rejection grade 1.

Table 3. Results of prediction by SVM, bagSVM and RF methods.

Method	Discovery Set modeling		Test Set prediction (+ 1 NSTA bx from discovery test)			
SVM	Accuracy (%):	100			**prediction**	
	Sensitivity (%):	100			STA	NSTA
	Specificity (%):	100	**actual**	STA	6	0
				NSTA	0	1
bagSVM	Accuracy (%):	100			**prediction**	
	Sensitivity (%):	100			STA	NSTA
	Specificity (%):	100	**actual**	STA	6	0
				NSTA	0	1
RF	Accuracy (%):	100			**prediction**	
	Sensitivity (%):	100			STA	NSTA
	Specificity (%):	100	**actual**	STA	5	1
				NSTA	0	1

SVM: Support vector machine / RF: Random forest